Phosphate recovery through struvite-family crystals precipitated in the presence of citric acid: mineralogical phase and morphology evaluation

by Luluk Edahwati

Submission date: 26-Nov-2020 09:07AM (UTC+0700)
Submission ID: 1457304211
File name: 3.2.Phosphate_recovery.pdf (2.09M)
Word count: 8454
Character count: 44123

Environmental Technology

ISSN: 0959-3330 (Print) 1479-487X (Online) Journal homepage: http://www.tandfonline.com/loi/tent20

Phosphate recovery through struvite-family crystals precipitated in the presence of citric acid: mineralogical phase and morphology evaluation

D. S. Perwitasari, L. Edahwati, S. Sutiyono, S. Muryanto, J. Jamari & A. P. Bayuseno

To cite this article: D. S. Perwitasari, L. Edahwati, S. Sutiyono, S. Muryanto, J. Jamari & A. P. Bayuseno (2017) Phosphate recovery through struvite-family crystals precipitated in the presence of citric acid: mineralogical phase and morphology evaluation, Environmental Technology, 38:22, 2844-2855, DOI: 10.1080/09593330.2017.1278795

To link to this article: https://doi.org/10.1080/09593330.2017.1278795

Accepted author version posted online: 04 Jan 2017.
Published online: 23 Jan 2017.

ENVIRONMENTAL TECHNOLOGY, 2017
VOL. 38, NO. 22, 2844–2855
http://dx.doi.org/10.1080/09593330.2017.1278795

Taylor & Francis
Taylor & Francis Group

Phosphate recovery through struvite-family crystals precipitated in the presence of citric acid: mineralogical phase and morphology evaluation

D. S. Perwitasari[a,b], L. Edahwati[a,b], S. Sutiyono[a,b], S. Muryanto[b,c], J. Jamari[b] and A. P. Bayuseno[b]

[a]Department of Chemical Engineering, Universitas Pembangunan Nasional 'Veteran' Jawa Timur, Surabaya, Indonesia; [b]Center for Waste Management, Department of Mechanical Engineering, Diponegoro University, Semarang, Indonesia; [c]Department of Chemical Engineering, UNTAG University, Semarang, Indonesia

ABSTRACT

Precipitation strategy of struvite-family crystals is presented in this paper to recover phosphate and potassium from a synthetic wastewater in the presence of citric acid at elevated temperature. The crystal-forming solutions were prepared from crystals of $MgCl_2$ and $NH_4H_2PO_4$ with a molar ratio of 1:1:1 for Mg^{+2}, NH_4^+, and PO_4^{-3}, and the citric acid ($C_6H_8O_7$) was prepared (1.00 and 20.00 ppm) from citric acid crystals. The Rietveld analysis of X-ray powder diffraction pattern confirmed a mixed product of struvite, struvite-(K), and newberyite crystallized at 30°C in the absence of citric acid. In the presence of citric acid at 30° and 40°C, an abundance of struvite and struvite-(K) were observed. A minute impurity of sylvite and potassium peroxide was unexpectedly found in certain precipitates. The crystal solids have irregular flake-shaped morphology, as shown by scanning electron microscopy micrograph. All parameters (citric acid, temperature, pH, Mg/P, and N/P) were deliberately arranged to control struvite-family crystals precipitation.

ARTICLE HISTORY
Received 5 September 2016
Accepted 31 December 2016

KEYWORDS
Precipitation; struvite-family crystals; citric acid; elevated temperature; XRPD Rietveld analysis

1. Introduction

Precipitation of phosphate minerals, namely struvite ($MgNH_4PO_4{\cdot}6H_2O$), occurs commonly in process pipes, pumps, and other industrial equipment [1,2]. This occurrence could lead to significant problems, as the mineral may form scale deposit and thus blocking the pipes. In contrast, engineered struvite precipitation could be carried out to the phosphate and ammonium compounds from effluent of urban wastewaters, liquid manure, and industrial organic waste streams [3]. The resulted struvite crystals may be used as either fertilizer or raw material for the production of phosphorus, and therefore the struvite precipitation is now becoming economically interesting [1].

Extensive research on struvite precipitation has been conducted with the aim at inhibiting scaling problems of pipelines including precipitation in tanks [2]. All reviews conducted *so far* have been focused on: (i) struvite solubility product of crystal dissolution patterns of both pure water and water solutions at controlled laboratory conditions [4]; (ii) understanding of the spontaneous struvite precipitation conditions based on the thermodynamic modeling of wastewater [5]; and (iii) modeling of struvite precipitation conditions for minimum struvite solubility by an approach of the pH solution [1]. *Struvite crystals* are generally *made* up of 9.8 wt.% magnesium, 7.3 wt.% ammonium, 38.8 wt.% phosphate, and 44.1% water and organic compounds [1]. Struvite usually precipitates as stable white orthorhombic crystals according to the following equation (with $n = 0$, 1, and 2) [1]:

$$Mg^{2+} + NH_4^+ + H_nPO_4^{n-3} + 6H_2O \rightarrow MgNH_4PO_4 \cdot 6(H_2O) + nH^+. \quad (1)$$

Struvite is only slightly soluble in water, but its solubility may be greatly enhanced in dilute acidic solutions [6]. Because it has low solubility in alkaline solution, the reaction solution may exhibit struvite precipitation. Moreover, factors controlling struvite crystallization in a piping system may include surface roughness of interior pipes. For example, slower precipitation of struvite may be found in the polyvinyl chloride (PVC), polyethylene plastic pipes, and PVC fittings, but higher, increasing struvite formation may take place in metal pipes [7]. Struvite precipitation may be influenced by an increase in energy caused by vibration or turbulent flow [3] and increasing pH from the released CO_2 as a result of pressure drop in pipes [8].

Further formation and crystal growth of struvite may be controlled by eliminating the driving force of the reaction or restricting the access of ionic species to the growing face of crystals. To some extent, struvite precipitation in the supersaturated solution can be adjusted by additives, which eventually control the characteristics of

CONTACT A. P. Bayuseno apbayuseno@gmail.com The Center for Waste Management, Mechanical Engineering Graduate Program, Diponegoro University, Tembalang Campus, Semarang 50275, Indonesia

the precipitating solid [5,9]. The presence of impurities may affect the growth rate of crystals by either blocking the active growth sites or incorporating into the crystal lattices. The blocking would result in the reduction of the growth of a particular crystal face relative to other faces. Meanwhile, the incorporation of the impurities into the crystal lattice may bring about distortion of the crystal shape [1,10]. Many foreign ions and compounds, including potassium, chloride, calcium, carbonates, copper, and zinc have been found to disturb crystal growth of struvite [11,12]. These ions may be absorbed on crystal surfaces and hence retarding struvite formation.

Struvite precipitated in the presence of foreign ions has gained great interest as a route to phosphorus recovery [1,8,13]. Due to the complexity and variety of mineralization processes, there are likely mineralogical differences in crystal growth by different foreign ions. However, only limited studies to date have focused on characterizing these similarities and differences. Efforts to investigate the long-term mineral stability process involved in these complex, in homogeneous, non-equilibrium systems require a complete chemical and mineralogical characterization (qualitative and quantitative) of precipitates [14,15]. Additionally, the quantitative mineralogical characterization is required for an efficient quality control in such variety of morphologies and purity of struvite crystals. These characterization results also offer significant insights into the ways for crystal growth at diverse natural and laboratory conditions [16].

The present work was undertaken to access the benefits of precipitation method on phosphate and potassium recovery from synthetic wastewater. The emphasis of this study was to explore the effects of organic acids as additives on the struvite-family crystals nucleation and growth, and discuss their impact on the quality of the recovered crystals. The degree of crystallinity and quantity of mineral products was analyzed by the Rietveld refinement method of the X-ray powder diffraction (XRPD). Scanning electron microscopy (SEM) equipped by energy dispersive X-ray analysis (EDX) was used to investigate the morphology and elemental analysis of the products. The precipitation experiment was done in a batch mode using a laboratory glass beaker, equipped with paraphernalia as required.

2. Materials and methods

2.1. Batch-precipitation experiments

Analytical grade chemicals (Merck™) or their equivalent were used without further purification. The stock solutions for the experiment were made by separately dissolving predetermined amounts of crystals of $MgCl_2$ and $NH_4H_2PO_4$ in double-distilled water to provide the struvite components, that is, Mg^{2+}, NH^{4+}, and PO_4^{-3}, respectively, at equimolar concentrations of 0.030 M.

In the present study, the magnesium concentrations were set up to obtain Mg:N:P equal to 1:1:1 [17]. It is very common that a low magnesium concentration relative to ammonia and phosphates is found in real wastewaters and here magnesium is usually added to affect the struvite crystallization process. In the present work, $MgCl_2$ was selected as a magnesium source in view of the result reported by Lee et al. [17], that is, due to its high solubility.

To ensure that the dissolved CO_2 did not interfere with the pH level of the precipitating solution, the double-distilled water was previously boiled and subsequently cooled for each solution preparation. The initial pH of both solutions was adjusted to 9.00 by drop-wise addition of 0.5 N KOH. It was important here to use alkali pH adjustment for ease struvite precipitation. The ions concentrations present in the prepared solutions in addition to K due to KOH addition was presented in Table 1.

The effect of citric acid (at 0.00, 1.00, and 20.00 ppm) on struvite precipitation was evaluated in this work. In this case, crystals of citric acid were diluted and added into $MgCl_2$ solution. Subsequently, equimolar solutions of $MgCl_2$ and $NH_4H_2PO_4$ were separately prepared in the glass beaker of 150 ml and each solution was then heated up to the desired temperature of 30°C and 40° C. The precipitation experiment was conducted by mixing the two solutions in a glass beaker of 500 ml. It was indicated that higher temperature of 40°C did not seem to instigate the evaporation of the ammonia (NH_3) in the solution [18]. The beaker was fitted with an agitator to provide stirring necessary for the homogenization of the solution. At the start of the run, the beaker was agitated vigorously for 10 s to ensure fast homogenization. Then, the stirring speed was reduced to 200 rpm until the end of the run. The speed of 200 rpm was chosen as preliminary experiment indicated that the speed could fully agitate the solution without any settling, or otherwise breakage, of the crystals formed.

The precipitation process was observed by continuously measuring the change in the pH level of the solution [11]. The pH meter was calibrated using ISO

Table 1. The approximate composition of the synthetic wastewater.

Parameter (molality)	PO_4	NH_4	Mg	K	Cl
Synthetic wastewater [mol/kg]	0.1829	0.3418	0.2040	0.2116	0.0964

standard buffers before each experiment. Due to the release of H^+ during precipitation (Equation (1)), the solution pH dropped continuously and started to tail off after approximately 70 min. Trial runs have shown that after 70 min the pH drop was negligible, hence it was decided that the run was terminated in 90 min. To assure repeatability, the experiments were performed in duplicate and the average values obtained were used. At the end of the precipitation run, the agitator was switched off and the beaker was gently decanted to quickly remove the precipitates. The recovered precipitates were then filtered and washed gently with distilled water, and subsequently air dried. The dried precipitates were stored in vials for further analysis. The washing procedure was somewhat offset by removing the co-precipitates. However, it was envisaged that chlorides and alkali ions were only chemical species that may be removed from the solution residue during washing [19], while struvite remained in the recovered products.

2.2. Chemical thermodynamic modeling

The Visual Minteq software program version 3.0 was employed to calculate the solution equilibrium model using the input data of ion concentrations in the synthetic wastewater [20]. The Visual Minteq was selected in the study to predict the mineral speciation formed in the solution. The chemical composition of the synthetic wastewater for the input of the program is given in Table 1. The model of mineral species was subsequently calculated by the program, using pH values and temperatures of 30°C and 40°C as input parameter. The mineral species predicted by the program were subsequently confirmed by the XRPD Rietveld method.

2.3. Materials characterization

The characterization of the precipitated crystals was performed through the XRPD method and SEM coupled with an energy dispersive X-ray analysis (SEM–EDX). The crystals obtained were ground with a pestle and mortar to obtain powder with sizes <75 µm. The ground powder was mounted in an aluminum sample holder for XRPD analysis. A Philips PW 1710 Diffractometer equipped with a Cu tube was applied for obtaining the XRPD data. Phase identification was made with (Powder Diffraction File) – PDF-2 Phillips software. Rietveld refinement of the XRPD data was carried out with Program Fullprof-2k, version 3.30 [21]. The relevant measured data used in the refinement are provided in Table 2.

The specimen-dependent parameters refined were (i) the 2θ scale zero position, (ii) the polynomial fitting for the background with six coefficients, (iii) the phase scale factors,(iv) the cell parameters, (v) the peak asymmetry and the peak shape functions, and (vi) the atomic coordinates and anisotropic temperature factors. The Fullprof fits the full-width at half-maximum of XRPD peak profiles as a function of tan (θ) using the u–v–w formula of Caglioti et al. [22], while u, v, and w were fixed to the values of the measured quartz. Preferred orientation of struvite was refined, while other phases were assumed to be absent in the powder precipitate in all cases. The obtained values of the cell parameters and the calculated weight% levels of mineralogical phases and the crystal structure models from which the full diffraction profiles are calculated by the program [14]. The calculation method is discussed in detail elsewhere [16].

Table 2. Measured data from XRPD used for the rietveld refinement.

Geometry	Bragg-Brentano
Goniometer radius	240 mm
Radius source	CuK_α
Generator	40 kV, 30 mA
Tube	Normal focus 10 × 1 mm
Divergence and receiving slits	0.2117°
Soiler slits	5.3°
Resolving slit	100 mm
Monochromator	Graphite (diffracted beam)
Detector	Scintillation counter
The scan parameters and step size	5–90° 2θ in 0.020° increments
Integration time	10 s

Furthermore, characterization of the samples was performed to investigate the morphology, elemental composition and crystal phases. For this purpose, SEM coupled with EDX and XRPD was utilized.

3. Results and discussion

3.1. Effects of the citric acid and temperature on the crystal growth of struvite

Figure 1(a) shows the decrease in pH both in the absence and in the presence of citric acid. As can be seen, pH drops sharply for the first 5 min, followed by a steady gradual reduction. Finally, the decrease tails off after approximately 70 min. As reported by Babic-Ivancic et al. [23], such a plateau decrease of pH indicates that struvite-family crystals (struvite and newberyite) may be formed.

The evolution of H^+ resulting from the precipitation reaction (Equation (1)) may have over-ridden the release of H^+ due to hydrolysis of citric acid, since (as common for organic acids) this acid is weak, that is, with a very low K_{sp}. In the both systems, the initial drop of pH was followed by a plateau, suggesting the dissolution and crystal growth of one or more crystals at

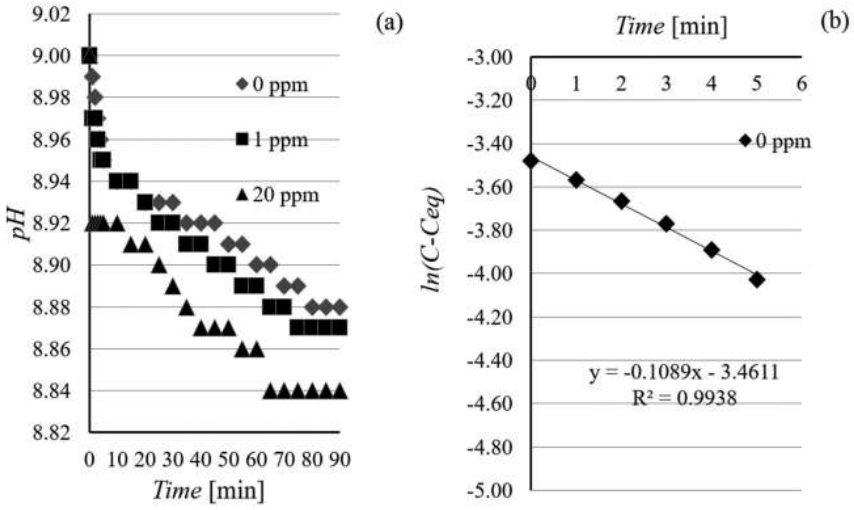

Figure 1. (a) Plot of pH reduction over time with and without additives at 30°C. (b) Curve fitting of the calculated $[Mg^{2+}]$ for the first-order kinetic in the absence of additives.

approximately constant supersaturation. During the precipitation process, ions of Mg^{+2}, NH_4^+, and PO_4^{-3} may form chemical species such as NH_3, NH_4^+, H_3PO_4, $H_2PO_4^-$, HPO_4^{-2}, $MgOH^+$, $MgNH_4PO_4$, $MgPO_4^-$, $MgH_2PO_4^+$, and $MgHPO_4$ and then control the pH level in aqueous system [9,12,24].

Further knowledge on kinetics of the precipitation is required for understanding the rates of struvite formation. Struvite precipitation kinetics may follow two major mechanisms: the nucleation and crystal growth [10]. The rate at which struvite precipitates corresponds to the interval of time required for the first particles to grow, more commonly known as induction time. In the present study, the growth rate of the crystals is not defined as linear growth rate and therefore does not have dimensions of length per unit time. Instead, the growth is characterized by the increase of the crystal mass, termed 'overall growth rates' and thus irrespective of the growth of the crystal faces [25,p. 52]. As shown in Equation (1), the precipitation of struvite liberates H^+ at the expense of Mg^{2+}, and thus pH of the solution decreases. Consequently, the precipitation rate can be determined by calculating the increase in $[H^+]$ as manifested by the pH decrease.

In this work, analysis of the crystallization process was based on the measured pH data onto the calculation of Mg^{2+} reduction, as described previously by Muryanto and Bayuseno [11]. From the previous observations, it was evident that the intensity of drop in pH was associated to the initial concentration of magnesium in solution and was characteristic of the speed at which the first crystals of struvite forms, thus to the rate of struvite precipitation. Moreover, a relationship between pH and Mg concentration against time can be used to predict kinetics of struvite precipitation and determine rate constants of struvite formation under specific condition of precipitation.

The change in concentration of $[Mg^{2+}]$ over time and the kinetic constants of struvite crystallization were calculated using a proposed kinetic model as follows [11]:

$$ln(C - C_{eq}) = -kt + ln(C - C_0),$$

where $C = [Mg^{2+}]$ at any time t (molar).

$C_{eq} = [Mg^{2+}]$ at equilibrium (molar).

C_0 = initial $[Mg^{2+}]$ at time zero ($t = 0$) (molar).

k = reaction rate constant (h^{-1}).

t = crystallization time (min).

Figure 1(b) presents the line of best fit for the typical experimental run of initial 6 min in the absence of additive and temperature of 30°C. It is shown that the reaction crystallization reasonably fits first-order kinetics model with correlation coefficient, R^2 of 0.9938. During 10–70 min, the reaction obeyed the first-order rate kinetic model with a regression coefficient value of 0.9452. Additionally, two phases of the kinetic were considered here and the values of the reaction rate constants in the presence of additives were similarly calculated from the slopes of the straight lines, and the values were listed in Table 3. It was observed from the experimental runs at 30°C and in the absence of the additive, the lines confirm the first-order rate equation, in which rate values of 1.776 and 6.534 h^{-1} agreed with the results of previous studies [12,24,26]. However, a low value of R^2 (0.8849 and 0.4286) for the first order

Table 3. The first-order rate constants for struvite crystallization.

		Intial period of 0–6 min			Period of 10–70 min		
		Regression equation	Rate constant (h^{-1})	R^2	Regression equation	Rate constant (h^{-1})	R^2
	200 rpm; $T = 30^{\circ}C$						
Additive	0.00 (ppm)	$y = -0.1089x - 3.4611$	6.534	0.9938	$y = -0.0296x - 3.6465$	1.776	0.9452
	1.00 (ppm)	$y = -0.0931x - 3.4851$	5.586	0.8849	$y = -0.0269x - 3.6580$	1.614	0.9611
	20.00 (ppm)	$y = -0.1017x - 3.5420$	6.102	0.4286	$y = -0.0268x - 3.6028$	1.608	0.9626
	200 rpm; $T = 40^{\circ}C$						
Additive	0.00 (ppm)	$y = -0.0861x - 3.1660$	5.166	0.9922	$y = -0.0283x - 3.2616$	1.698	0.9656
	1.00 (ppm)	$y = -0.0771x - 3.1016$	4.626	0.7709	$y = -0.0258x - 3.2268$	1.548	0.9389
	20.00 (ppm)	$y = -0.0783x - 3.0553$	4.698	0.4286	$y = -0.0222x - 3.2829$	1.332	0.9302

of the experimental run in the presence of additives (1 and 20 ppm) was observed at the initial 6 min. The reason for this rather contradictory result may be due to the agitation speed, which may have erroneously fluctuated, hence bringing about uneven changes in pH. In the presence of additives, the subsequent crystallization process (10–70 min) still obeyed the first order of kinetic with regression values of 0.9611 and 0.9626, respectively. This indicates that the rate of reaction depended on the presence of additives for change of Mg^{2+} concentration present in the solution.

Furthermore, the amount of additives and rate constants was observed to be negatively correlated. This result also agreed with previous finding on crystallization reaction [27]. In this case, the additives added were shown to retard the overall mass growth rate. The decrease in reaction rates was manifested in the reduction of crystal growth. Consequently, in the period of 10–70 min, the maximum inhibition of crystal growth can be calculated based on the different data of between the highest (0 ppm) and the lowest rates (20 ppm) as follows: $[(1.776–1.608)/1.776] \times 100\% = 9.4\%$.

The formation of struvite highly depends on the level of supersaturation of the precipitating solution. Furthermore, the supersaturation level can be expressed in terms of saturation index (SI), which equals log [IAP/K_{sp}]. In this term, IAP represents the ion activity product of struvite species, that is, Mg^{2+}, NH_4^+, and $PO_4^{3}-$; whereas K_{sp} is the solubility product of struvite. In the present study, the calculated SIs of the various solid phases are presented in Table 4. Also, SI was used to predict the saturation state of precipitating system. If SI > 0, the solution is supersaturated and precipitation may occur spontaneously; If SI = 0, the solution is in equilibrium; If SI < 0, the solution is under saturated and no precipitation may occur.

Minteq predicted that the SI values for farringtonite, newberyite, struvite, and struvite (K) were above zero in the pH 9. Therefore, newberyite, struvite, and struvite (K) were predicted to precipitate from the solution. In the wastewater system, struvite can be formed at neutral and higher pH, while newberyite precipitation occurs at lower pH (pH < 6) [9,12,24]. Nevertheless, the crystallization of farringtonite may take place in the order of days [28]. Thus, this mineral was predicted to be absent in the precipitate.

All other minerals [$Mg(OH)_2$, $Mg_2(OH)_3Cl{\cdot}4H_2O$, periclase, and sylvite] were undersaturated, consequently they would not crystallize. Apparently, several processes (nucleation, crystal growth, and dissolution of some minerals) were included in the calculation taking place simultaneously. The processes responsible for the specific mineral formation may be unidentified in the present work.

With increasing temperature to 40°C and in the absence of citric acid, an immediate pronounced drop of pH, from an initial value of 9 to approximately 8.90 < pH < 8.95 was observed, providing a fast precipitation of 5 min (Figure 2(a)). Then it was followed by a slight and gradual decrease of pH and finally leveled off and reach equilibrium at pH 8.8. By adding 1.00 and 20.00 ppm of citric acids, the precipitation time prolonged. Later, a gradual pH reduction over time was shown for all systems and ended at 90 min. The decreased pH appears as a consequence of the precipitation of some minerals. During these precipitation processes, the dissolution and crystal growth of two or more struvite-family crystals may occur simultaneously [23].

The typical reaction order for struvite crystallization in the absence of citric acid at a temperature of 40°C is shown in Figure 2(b). As can be seen in the initial 6 min, the reaction crystallization reasonably fits

Table 4. Mineral species predicted from the visual minteq model.

	Solution at pH = 9 $T = 30^{\circ}C$		Solution at pH = 9 $T = 40^{\circ}C$	
Mineral species	Log IAP	SI	Log IAP	SI
Sylvite	−1.86	−2.76	−1.86	−2.76
$Mg(OH)_2$	16.47	−2.32	16.46	−2.34
$Mg_2(OH)_3Cl{\cdot}4H_2O$	22.83	−3.16	22.81	−3.19
Farringtonite	−15.49	7.79	−15.48	7.81
Newberyite	−15.98	2.19	−15.97	2.21
Periclase	16.47	−4.67	16.46	−3.86
Struvite	−7.72	5.55	−7.86	5.41
Struvite (K)	−7.73	2.89	−7.72	2.91

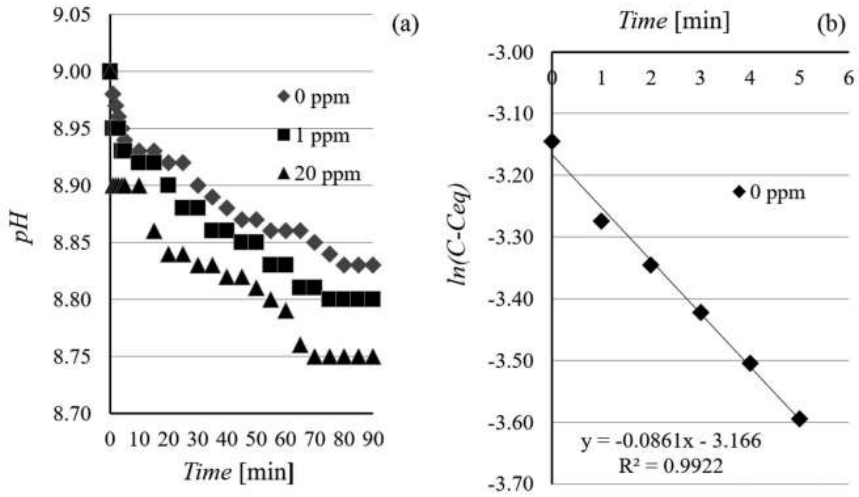

Figure 2. (a) Plot of pH reduction over time with and without additives at 40°C. (b) Curve fitting of the calculated [Mg^{2+}] for the first-order kinetic in the absence of additives.

first-order kinetics model with correlation coefficient, R^2 of 0.9902. The low value result of regression coefficient was also obtained from the typical reaction in the presence of additives (1 and 20 ppm). However, the best fit of lines for the reaction was observed for all experimental runs after 10 min ($R^2 = 0.9656$, 0.9389 and 0.9302). The reaction rate constants of the experimental runs in the absence and the presence of additives at 40°C, as obtained from the slopes of the lines of best fit were 1.698, 1.548, and 1.332 h^{-1} respectively; which were in close agreement with the values obtained for 30°C (Table 3). It was proposed that first-order growth rate happened in two phases and the results showed no significant dependence on temperature, but on pH.

The struvite growth rate against the change of temperature has been also demonstrated previously [29]. The struvite growth has been suggested to increase in the temperature range of 25–35°C and subsequently decreases at 40°C [29]. The type of crystals could be subsequently predicted from SI-containing minerals (Table 4). At 40°C, farringtonite, newberyite, struvite, and struvite (K) may be formed at pH solution of 9, whereas other minerals (brushite, sylvite, $Mg(OH)_2$, $Mg_2(OH)_3Cl{\cdot}4H_2O$, and periclase) were undersaturated and not predicted to precipitate in the solution.

Furthermore, the pH reduction of 9 to approximately 8.5, promoted the increasing concentration of phosphate ions, which has been reported to be predominantly HPO_4^{2-} [30]. In contrast to more phosphate ions present in the solution due to the pH increasing, the reduction of concentrations of Mg and NH_4 may be followed for establishing a range of solubility limits. The high phosphorus removal efficiency may be completed by increasing pH from 7.6 to 8.5 [24]. Nevertheless, the pattern of mineral formation for phosphate recovery was rather complicated in the precipitation system observed in the study. This is because the dissolution of struvite and newberyite may have simultaneously taken in the limited range of supersaturation [9].

3.2. Mineralogical characterization of the precipitating solids

Initially, the classical (albeit *computerized*) XRPD search-match method found that the XRPD patterns of the precipitating solid with no additive matched with PDF#71-2089 for struvite; the PDF#35-0812 for struvite-(K) [$KMgPO_4{\cdot}6H_2O$]; PDF#70-2345 for newberyite [$MgHPO_4{\cdot}3H_2O$]; and PDF#76-3368 for sylvite (KCl). Those minerals was subsequently judged by the full-profile Rietveld refinement, as the peaks of phases which have been overlapped in the search match or mistakenly assigned phases clearly stand out in the difference plot of the calculated and the measured diffraction profile [15,31]. The quality of refinements of the solid in the absence of additive, taken as an example, may be gaged from the diffraction plot in Figure 3(A). The intensity of most peaks is well represented in the calculated diffractogram. The XRPD analysis also confirmed the crystalline nature of the precipitates, since no significant amorphous phase as can be seen from the background profile.

X-ray diffractograms of the precipitating solids with a variation of additive concentrations are shown in Figure 3(B). Each peak had been judged by the full-profile Rietveld refinement and labeled with the mineralogical

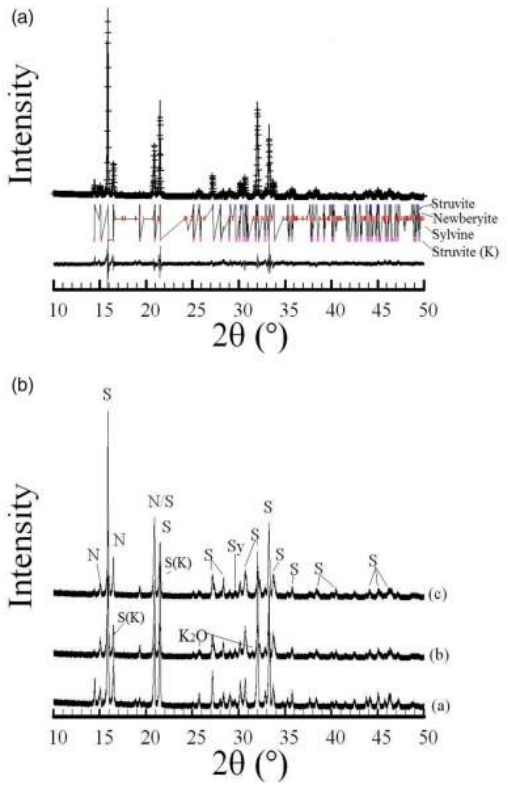

Figure 3. (a) Plot of XRPD Rietveld analysis of the crystals precipitated in the absence of additives at 30°C. (B) XRPD patterns of the precipitates with (a) 0, (b) 1, and (c) 20 ppm citric acid. The principal diffraction peaks of the predominant minerals are shown for reference purposes. The peaks are labeled N (newberyite), S (struvite), S-(K) (struvite-K), and Sy (sylvite).

phase name. The XRPD signals provided direct the experimental evidence of the struvite and struvite-(K) minerals formed in the precipitating solid [32]. In particular, the precipitates obtained with no additives showed peaks of sylvite and newberyite. Crystal growth of sylvite in the precipitate could be attributed to the precipitation of excessive potassium reacted with chloride ions and was subsequently formed during the drying.

The further addition of 1 and 20 ppm citric acids in the solution at the temperature of 30°C, struvite-(K) was found, as can be estimated from the peaks at 20.932 2θ° (PDF#35-0812), in addition to minerals of struvite and sylvite. The XRPD pattern of struvite-(K) was identical and identified a close relationship to the mineral struvite. The patterns of struvite and struvite-(K) are quite similar and overlapped, but the complicated patterns could be practically distinguished during the XRPD Rietveld analysis. Taking the positions of other peaks into account, struvite-(K) seems to be the most likely mineral commonly found as the natural potassium equivalent of struvite [33,34]. Moreover, an oxide mineral close to potassium peroxide [KO_2] was formed in the precipitate with 1 ppm additive and could be verified in the XRPD trace at 31.342 2θ° (PDF# 89-5955) [35]. The formation of this mineral may be related to K-ion from KOH, which subsequently reacted with oxygen during drying. However, KO_2 was not identified in the precipitate with 20 ppm additive. The reason for the absence of KO_2 at 20 ppm of citric acid is not easy to explain but it can be argued that the limiting reagent of O_2 can be the source of these differences.

The formation of struvite-family crystals at the temperature of 30°C was also confirmed by SEM/EDX analysis. An irregular flake-shaped morphology was shown in the crystalline solid without and with additives. They were a typical mixture of crystalline struvite-family crystals (Figure 4(a–c)) [33,36]. The resulting struvite and struvite-(K) structures may be predicted from the presence of these ions: K^+, Mg^{2+}, N^{5+}, O^{2-}, and P^{5+}, as shown by the EDX spectrum (Figure 4(a–c)). Mg^{2+}, O^{2-}, and P^{5+} could be responsible for the newberyite, while K^+ and Cl^- for sylvite.

Similarly, XRPD patterns of the resulting samples added with 1 and 20 ppm citric acids at 40°C are shown in Figure 5. In the precipitates obtained with no additive, peaks of struvite, struvite-(K), and sylvite were clearly identified, but peaks of newberyite disappeared. Up to the citric acid addition of 20 ppm, a mixed crystal of struvite, struvite-(K), and sylvite precipitated out the solution. With increasing temperature, mineralogical phase compositions of the solid were altered as a result of the chemical equilibrium of some ions (i.e. magnesium, ammonium, and phosphate) [24]. The increasing temperature may also be favor for the fast reaction rate, hence resulting in the increased 'K' precipitation. Clearly, the forms of struvite and struvite-(K) were the main phases precipitated out the solution at 40°C.

The mixed product of struvite and struvite-(K) precipitated out the solution at 40°C in the absence and the presence of additives could be confirmed by SEM analysis. Irregular flake-shaped crystals formed into the precipitate are shown in Figure 6(a–c). The most common elements identified with EDX in the precipitating solids are K^+, Mg^{2+}, N^{5+}, O_2^-, and P^{5+} in agreement with the compositions of struvite and struvite-(K) (Figure 6(a–c)). This crystal solid may also accommodate cation K^+ and anion Cl^- as a composition of sylvite mineral.

Quantity of struvite crystals formed into the precipitating process was evaluated by the XRPD Rietveld method using the crystal structures model present in the literatures (Table 5). It is suggested here that the quantitative values (wt.%) shown in Table 5 was XRPD-based quantitative analysis, while the EDX data only

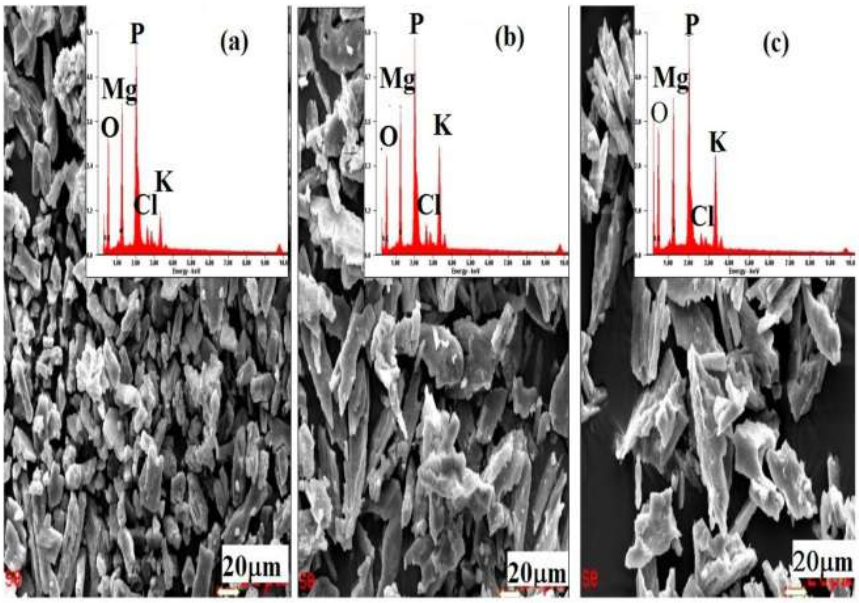

Figure 4. SEM image of a flake-shaped crystal morphology and EDX spectrum obtained from the precipitates at 30°C in the presence of (a) 0, (b) 1, and (c) 20 ppm citric acid.

provided their characteristics dispersive X-ray spectra of elements (i.e. P, Mg, K, and O) in the crystals. The XRPD Rietveld analysis confirmed that each unit cell parameter calculated for each mineral were closer to the data of reported values.

With no additive used, there is an evidence for the major formation of the struvite (63.3 wt.%) and struvite-(K) (30.4 wt.%), but the minor minerals of newberyite (5.5 wt.%) and sylvite (0.8 wt.%). A decreased amount of struvite was observed as a result of the citric acid addition at 1 and 20 ppm, compared to those in the previous precipitating solids. Struvite-(K) was yet formed into increasing additives, but newberyite disappeared. This is because newberyite is commonly unstable at pH > 6.5 [37]. Moreover, the major phase arising out of the solution to 1 ppm additive was to be struvite (72.1 wt.%) and struvite-(K) (26.8 wt.%), but only minor impurities of sylvite (0.63 wt.%) and potassium peroxide (0.80 wt.%) were unexpectedly produced. Similarly, the major phases such as struvite (73.2 wt.%) and struvite-(K) (26.2 wt.%) were found in the precipitating solids with 20 ppm additive, while the minor amount of sylvite was still developing.

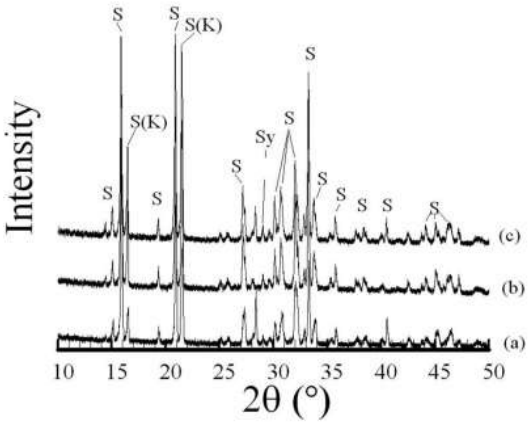

Figure 5. XRPD patterns of the precipitates with (a) 0, (b) 1, and (c) 20 ppm citric acid at 40°C. The principal diffraction peaks of the predominant minerals are shown for reference purposes. The peaks are labeled S (struvite), S(K) (struvite-K), and Sy (sylvite).

Insignificant changes in the amounts of struvite and struvite-(K) with the increasing temperature were also noticed. As the temperature of 40°C and no citric acid added, amounts of struvite (71.8 wt.%) and struvite-(K) (22.8 wt.%) were produced, while the amount of minor sylvite (5.4 wt.%) was obtained. Moreover, the addition of 1 ppm citric acid in the solution yielded a relative abundance of struvite (66.2 wt.%) and struvite-(K) (33.7 wt.%). Using 20 ppm additive, the major phases for struvite (77.2 wt.%), struvite-(K) (21.5 wt.%), and minor of sylvite was produced. In this study, struvite may be precipitated by consuming high content of ammonium (NH_4^+) present in the solution. With initial solution concentrations of magnesium (Mg^{2+}), ammonium (NH^{4+}), and phosphate (PO_4^{3-}) (MAP) at a molar ratio of 1:1:1, the concentration of ammonium (NH^{4+}) decreased,

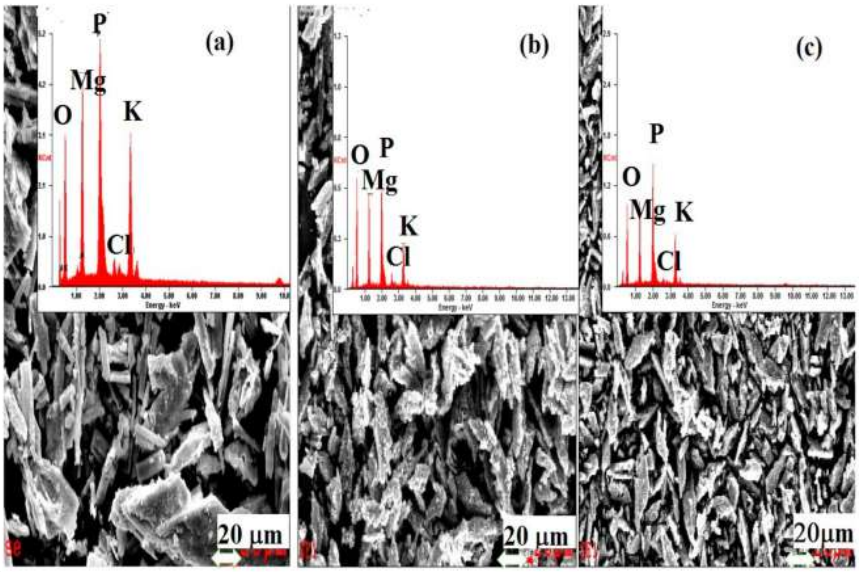

Figure 6. SEM image of a flake-shaped crystal morphology and EDX spectrum obtained from the precipitates at 40°C in the presence of (a) 0, (b) 1, and (c) 20 ppm.

once the struvite crystals formed, which indicated that a precipitate was composed of struvite and struvite-(K). This MAP molar ratio of 1:1:1 has been also regarded to be the approximate minimum required for struvite precipitation [5].

3.3. Effect of additives on the morphology of precipitates

Figure 4 presents the type of morphology for struvite-family crystals precipitated in the absence and the presence of the citric acids at 30°C. The irregular flake-shaped crystals about 20 µm in size were observed, whereas the crystals precipitated in the presence of citric acid exhibited larger size. Because of the spontaneous precipitation, some elongated crystals developed, compared with the crystals obtained by spontaneous precipitation in the absence of additives [13].

The work of Chauhan and Joshi [38] was carried using a gel growth method with the intention to investigate the growth of individual faces of a single crystal. It is well recognized that the gel growth method was primarily used to obtain crystals with good shape. In contrast, our work focuses on growth of crystals without specific attention to the growth of their individual faces. As can be pointed out from the work of Chauhan and Joshi [38], the different shapes obtained were the direct influence of the varying citric acid concentrations used. In that case, our work was in fact similar to Chauhan and Joshi [38].

In the presence and the absence of the citric acid additives at 40°C, the same morphology of crystals was discovered (Figure 6). All the same, the longer and thinner flake-shaped crystals in a size of about 60 µm long and 2 µm wide were mostly observed in the precipitate with no additive (Figure 6(a–c)). These results are consistent with the findings in the literature concerning the effects of pH on struvite morphology, suggesting that the irregular flake-shaped morphology is commonly formed into mildly alkaline conditions selected in the study [30,36]. Figure 4(a) depicts the struvite obtained at 30°C in the absence of citric acid, while Figure 6(a)

Table 5. XRPD-based mineralogy of the precipitates obtained at initial pH 9 and the elevated temperature for mixing speed of 200 rpm.

		Concentration of the additive and the solution temperature of 30°C			Concentration of the additive and the solution temperature of 40°C			
Mineral (wt.%)	Formula	0 ppm	1 ppm	20 ppm	0 ppm	1 ppm	20 ppm	The crystal structure model
Struvite	$MgNH_4PO_4{\cdot}6H_2O$	63.3 (7)	72.1 (5)	73.2 (8)	62.7 (5)	66.2 (6)	77.2 (9)	Whitaker and Jeffery [32]
Struvite-K	$KMgPO4{\cdot}6H_2O$	30.4 (8)	26.8 (6)	26.2 (9)	31.2 (6)	33.2 (6)	21.5 (4)	Graeser et al. [33]
Newberyite	$MgHPO_4{\cdot}3H_2O$	5.5 (2)	–	–		–		Abbona et al. [46]
Sylvite	KCl	0.8 (4)	0.3 (1)	0.6 (2)	6.1 (1)	0.6 (4)	1.3 (4)	Ott [48]
Potassium peroxide	KO_2		0.8 (6)					Ziegler et al. [35]

Note: Figures in parentheses indicate the least-squares estimated standard deviation referring to the least significant figure to left.

shows the struvite crystals obtained at 40°C under otherwise the same conditions as in Figure 4(a). It could be postulated therefore that higher temperature brings about elongation of the crystals. That temperature influences crystal shape is also common. For example, Babic-Ivancic et al. [23] reported that different temperatures lead to different morphologies.

Furthermore, firstly, our research focuses on precipitation of struvite as impacted by several selected parameters. We do not emphasize on crystal engineering, that is, on detailed crystal shape as defined by morphology or crystal habit. A number of papers on precipitation also present the issue of morphology in this sense [10]. Secondly, it is true that in our work the obtained crystals are very irregular, but it can be roughly described as plate-like especially as shown in Figure 6(a), that is, under elevated temperature of 40°C. Similar results can be seen in the work of Mehta and Batstone [39]; Tao et al. [40], and Romero-Guiza et al. [41]. In theories of crystal growth, the morphology of crystals can be influenced by the slow-growing faces because of the possibility of disappearing in the fast-growing faces which are not represented in the final habit. However, it was recently reported that the morphological importance of faces cannot be inversely proportional to their growth rates [10]. It was indicated that this acid may affect fundamental precipitation aspects, particularly nucleation and growth [42–44].

As demonstrated by previous studies, the morphology of struvite crystals and growth process are strongly controlled by the pH value [10]. By altering the pH solution, two or more struvite-family crystals with different morphologies was observed in the present study. The mechanism of such morphological changes may not be distinctly seen. However, it seems that crystallographic interaction may have an important role in such modification.

3.4. Findings of the study

In the present study, combination of nucleation and growth mechanism may apparently have occurred in two or more minerals. Nevertheless, the exact contribution to the overall kinetics of any of the particular mechanisms involved in the processes (nucleation, crystal growth of struvite-family crystal, and dissolution of them) could not be determined, because several phases were simultaneously present in the system. Moreover, the effective struvite precipitation could be achieved at pH values of 8.5 or greater [1,8]. The phosphate ions may be effectively converted into struvite and struvite-(K) at pH values examined [12,45]. A method of the increasing pH is necessary to optimize the struvite precipitation. One possible method to increase the pH would be by adding KOH, although other alkaline chemicals may be used. Additionally, the presence of excess of potassium ions in the solution may result in increasing the formation of struvite-(K) as observed in the present study.

Temperature may influence the precipitation of struvite. Depending on the precipitation parameters selected, the precipitation of struvite may recover a substantial amount of ammonium from wastewater [1,29]. As reported, struvite may precipitate alongside its family-crystals, that is,. struvite-(K) and newberyite, and therefore has the potential for resource recovery of magnesium, nitrogen, and phosphorus from wastewater [33,37,46,47].

Furthermore, qualitative and quantitative results of multiple minerals are important to reliably describe major minerals controlling MAP ions recovery from the solution. Because of the complexity of the mineralogy of the precipitates, using XRPD usually give only a qualitative mineralogical composition [11,13]. Use of conventional XRPD methods of multiphase identification of the precipitating solid has sometimes left some number of peaks to be unresolved. Moreover, the identity of many complex phases and the abundance of uncommon minerals remain uncertain. The XRPD Rietveld method is widely known as a comprehensive, computer-based method for the analysis of whole powder diffraction pattern, reducing the problem of extensive overlap between the strong peaks of many of the phases [14,15,49]. The method has already become a very practical and quick routine for standardless quantitative phase analysis of inorganic and cementious materials [16,50]. In the present study, the XRPD Rietveld technique could overcome many of the limitations of conventional XRPD for mineralogical quantitative evaluation because the method relies on the availability of a reliable database of phases in a mineral.

4. Conclusions

It can be concluded that a mixture of struvite, struvite-(K), and newberyite was the minerals controlling MAP and K-ions recovery at 30°C and initial pH 9. The abundance of struvite and struvite-(K) precipitated with citric acid at the same temperature. In the presence of additives at 40°C, struvite and struvite-(K) precipitated controlling MAP and K-ions recovery. The minor impurity of sylvite were formed into all precipitating solids, but only minor of potassium peroxide was found in certain precipitates. Struvite-family crystals were grown from the solution of artificial wastewater in the absence and the presence of citric acid. From this study, it can be

observed that in the absence of citric acid, the crystals in most cases take the irregular flake-shaped morphology, but the crystals of other needle like-habits were also observed in the presence of additives. Moreover, the differences in results were detected in their sizes.

Disclosure statement

No potential conflict of interest was reported by the authors.

Funding

The study was supported by Universitas Pembangunan Nasional 'Veteran' Jawa Timur, Surabaya, Indonesia under the PhD research grant programs.

References

[1] Doyle JD, Parsons SA. Struvite formation, control and recovery. Water Res. 2002;36:3925–3940.
[2] Capdeviellea A, Sykorová E, Biscans B, et al. Optimization of struvite precipitation in synthetic biologically treated swine wastewater-Determination of the optimal process parameters. J Hazard Mater. 2013;244–245:357–369.
[3] Wilsenach J, Schuurbiers C, van Loosdrecht MCM. Phosphate and potassium recovery from source separated urine through struvite precipitation. Water Res. 2007;41:458–466.
[4] Mehta CM, Batstone DJ. Nucleation and growth kinetics of struvite precipitation. Water Res. 2013;47:2890–2900.
[5] Stratful I, Scrimshaw MD, Lester JN. Conditions influencing the precipitation of magnesium ammonium phosphate. Water Res. 2001;35:4191–4199.
[6] Muench EV, Barr K. Controlled struvite precipitation for removing phosphorus from anaerobic digester side streams. Water Res. 2001;35:151–159.
[7] Ye ZL, Chen SH, Wang SM, et al. Phosphorus recovery from synthetic swine wastewater by chemical precipitation using response surface methodology. J Hazard Mater. 2010;176:1083–1088.
[8] Mohajit X, Bhattarai KK, Taiganides EP, et al. Struvite deposits in pipes and aerators. Biol Waste. 1989;30:133–147.
[9] Bouropoulos CHN, Koutsoukos PG. Spontaneous precipitation of struvite from aqueous solutions. J Cryst Growth. 2000;213:381–388.
[10] Prywer J, Olszynski M. Influence of disodium EDTA on the nucleation and growth of struvite and carbonate apatite. J Cryst Growth. 2013;375:108–114.
[11] Muryanto S, Bayuseno AP. Influence of Cu^{2+} and Zn^{2+} as additives on precipitation kinetics and morphology of struvite. Powder Technol. 2014;253:602–607.
[12] Ohlinger KN, Young TM, Schroeder ED. Postdigestion struvite precipitation using a fluidized bed reactor. J Environ Eng. 2000;126:361–368.
[13] Kofina AN, Demadis KD, Koutsoukos PG. The Effect of citric acid and phosphocitric acid on struvite spontaneous precipitation. Cryst Growth Des. 2007;7:2705–2712.
[14] Hill RJ, Howard CJ. Quantitative phase analysis from neutron powder diffraction data using the Rietveld method. J Appl Crystallogr. 1987;20:467–474.
[15] Rietveld HM. A profile refinement method for nuclear and magnetic structures. J Appl Crystallogr. 1969;2:65–71. doi:10.1107/S0021889869006558
[16] Bayuseno AP, Schmahl WW. Improved understanding of the pozzolanic behaviour of MSWI fly ash with $Ca(OH)_2$ solution. Int J Environ Waste Manage. 2015;15:39–66.
[17] Lee SI, Weon SY, Lee CW, et al. Removal of nitrogen and phosphate from wastewater by addition of bittern. Chemosphere. 2003;51:265–271.
[18] Harrison ML, Johns MR, White ET, et al. Growth rate kinetics for struvite crystallization. Chem Eng Trans. 2011;25:309–314.
[19] Bayuseno AP, Schmahl WW. Characterisation of MSWI fly ash through mineralogy and water extraction. Resour Conserv Recy. 2011;55:524–534.
[20] USEPA. A geochemical assessment model for environmental systems: version 3.0 user manual.U.S.EPA.EPA/600/3-91/021. Washington (DC) 1991.
[21] Rodriguez-Carvajal J. Program Fullprof 2k, version 3.30, Laboratoire Leon Brillouin, France, June 2005.
[22] Caglioti G, Paoletti A, Ricci FP. Choice of collimator for a crystal spectrometer for neutron diffraction. Nuclear Instrument. 1958;35:223–228.
[23] Babic-Ivančic V, Kontrec J, Brečevic L, et al. Kinetics of struvite to newberyite transformation in the precipitation system $MgCl_2$-$NH_4H_2PO_4$-NaO-H_2O. Water Res. 2006;40:3447–3455.
[24] Nelson NO, Mikkelsen RL, Hesterberg DL. Struvite precipitation in anaerobic swine lagoon liquid: effect of pH and Mg: P ratio and determination of rate constant. Bioresource Technol. 2003;89:229–236.
[25] Myerson AS. Molecular modeling applications in crystallization. Cambridge University Press, 1993.
[26] Ali I, Schneider P. An approach of estimating struvite growth kinetic incorporating thermodynamic and solution chemistry, kinetic and process description. Chem Eng Sci. 2008;63:3514–3525.
[27] Hoang TA, Ang HM, Rohl AL. Effects of organic additives on calcium sulfate scaling in pipes. Aust J Chem. 2009;62:927–933.
[28] Mamais D, Pitt PA, Cheng YW, et al. Determination of ferric chloride dose to control struvite precipitation in anaerobic sludge digesters, Water. Environ. Res. 1994;66:912–918.
[29] Bhuiyan MIH, Mavinic DS, Beckie RD. A solubility and thermodynamic study of struvite. Environ. Technol. 2007;28:1015–1026.
[30] Mijangos F, Kamel M, Lesmes G, et al. Synthesis of struvite by ion exchange isothermal supersaturation technique, reactive and functional polymers. 2004;60:151–161.
[31] Prince E. Mathematical aspects of rietveld refinement. The rietveld method. Edited by Young RA. International Union of Crystallography, Oxford, New York, 43–54 (1993).
[32] Whitaker A, Jeffery JW. The crystal structure of struvite, MgNH4PO4·6H2O. Acta Crystallogr. 1970;B26:1429–1440. doi:10.1107/S0567740870004284
[33] Graeser S, Postl W, Bojar HP, et al. Struvite-(K), $KMgPO_4$·$6H_2O$, the potassium equivalent of struvite a new mineral. Eur. J. Mineral. 2008;20:629–633.
[34] Chauhan CK, Vyas PM, Joshi MJ. Growth and characterization of Struvite-K crystals. Cryst. Res. Technol. 2011;46:187–194.

[35] Ziegler M, Rosenfeld M, Kanzig W, et al. Struktur untersuchungen an Alkalihyperoxiden. Helvetica Physica Acta. 1976;49:57–59.
[36] Kim BU, Lee WH, Lee HJ, et al. Ammonium nitrogen removal from slurry-type swine wastewater by pretreatment using struvite crystallization for nitrogen control of anaerobic digestion. Water Sci Technol. 2004;49:215–222.
[37] Abbona F, Lundager H, Madsen E, et al. The final phases of calcium and magnesium phosphates precipitated from solutions of high to medium concentration. J Cryst Growth. 1988;89:592–602.
[38] Chauhan CK, Joshi MJ. Growth inhibition of struvite crystals in the presence of juice of *Citrus medica* Linn. Urol Res. 2008;36:265–273.
[39] Mehta CM, Batstone DJ. Nucleation and growth kinetics of struvite crystallization. Water Res. 2013;47:2890–2900.
[40] Tao W, Fattah KP, Huchzermeier MP. Struvite recovery from anaerobically digested dairy manure: a review of application potential and hindrances. J Environ Manag. 2016;169:46–57.
[41] Romero-Guiza MS, Astals S, Mata-Alvarez J, et al. Feasibility of coupling anaerobic digestion and struvite precipitation in the same reactor: evaluation of different magnesium sources. Chem Eng J. 2015;270:542–548.
[42] Chauhan CK, Joshi MJ. In vitro crystallization, characterization and growth-inhibition study of urinary type struvite crystals. J Cryst Growth. 2013;362:330–337.
[43] Parekh BB, Joshi MJ. Crystal growth and dissolution of brushite crystals by different concentration of citric acid solutions. Indian J Pure Appl Phys. 2005;43:675–678.
[44] Joshi VS, Joshi MJ. Influence of inhibition of citric acid and lemon juice to the growth of calcium hydrogen phosphate dihydrate urinary crystals. Indian J Pure Appl Phys. 2003;41:183–192.
[45] Wang J, Burken JG, Zhang XJ. Effect of seeding materials and mixing strength on struvite precipitation. Water Env Res. 2006;78:125–132.
[46] Abbona F, Boistelle R, Haser R. Hydrogen bonding in $MgHPO_4{\cdot}3H_2O$ (newberyite). Acta Crystallogr. 1979; B35:2514–2518.
[47] Kontrec J, Babić-Ivančić V, Brečević L. Formation and morphology of struvite and newberyite in aqueous solutions at 25 and 37°C. Coll Antropol. 2005;29:289–294.
[48] Ott H. Die Strukturen von Mn O, Mn S, Ag F, Ni S, Sn I4, Sr Cl_2, Ba F_2, praezisions messungen einiger alkalihalogenide. Z Kristallogr. 1926;63:222–230.
[49] Winburn RS, Grier DG, McCarthy GJ, Peterson RB. Rietveld quantitative X-ray diffraction analysis of NIST fly ash standard reference materials. Powder Diff. 2000;15:163–172.
[50] Mahieux P-Y, Aubert J-E, Cyr M, Coutand M, Husson B. Quantitative mineralogical composition of complex mineral wastes – contribution of the Rietveld method. Waste Manage. 2010;30:378–388.

Phosphate recovery through struvite-family crystals precipitated in the presence of citric acid: mineralogical phase and morphology evaluation

ORIGINALITY REPORT

13%	12%	11%	4%
SIMILARITY INDEX	INTERNET SOURCES	PUBLICATIONS	STUDENT PAPERS

PRIMARY SOURCES

1	www.matec-conferences.org Internet Source	5%
2	eprints.undip.ac.id Internet Source	4%
3	worldwidescience.org Internet Source	2%
4	Athanasius Priharyoto Bayuseno, Dyah Suci Perwitasari, Stefanus Muryanto, Mohammad Tauviqirrahman, Jamari Jamari. "Kinetics and morphological characteristics of struvite (MgNH4PO4.6H2O) under the influence of maleic acid", Heliyon, 2020 Publication	2%

Exclude quotes	On	Exclude matches	< 2%
Exclude bibliography	On		

Phosphate recovery through struvite-family crystals precipitated in the presence of citric acid: mineralogical phase and morphology evaluation

GRADEMARK REPORT

FINAL GRADE

/0

GENERAL COMMENTS

Instructor

PAGE 1

PAGE 2

PAGE 3

PAGE 4

PAGE 5

PAGE 6

PAGE 7

PAGE 8

PAGE 9

PAGE 10

PAGE 11

PAGE 12

PAGE 13